

# A Novel Direct Control Procedure for an Interior Permanent Magnet Synchronous Generator Based Wind Turbine with Variable Speed

Sameer Sayed<sup>1</sup> | Shaik Hameed<sup>2</sup>

<sup>1</sup>PG Scholar, Department of EEE, Quba College of Engineering and Technology, Nellore, Andhra Pradesh, India.

<sup>2</sup>Associate Professor, Department of EEE, Quba College of Engineering and Technology, Nellore, Andhra Pradesh, India.

## To Cite this Article

Sameer Sayed and Shaik Hameed, "A Novel Direct Control Procedure for an Interior Permanent Magnet Synchronous Generator Based Wind Turbine with Variable Speed", *International Journal for Modern Trends in Science and Technology*, Vol. 03, Issue 07, July 2017, pp. 18-26.

## ABSTRACT

*This paper proposes a novel direct control policy for an interior permanent magnet synchronous generator-based wind turbine with variable speed. In this system, the condition of the incessant rotor place is eliminated as all the calculation is finished in the stator orientation casing. This method possesses reward such as smaller constraint reliance and abridged digit of controller compare among the conventional indirect vector control method. The direct control design is simpler and can eradicate some of the drawback of established indirect vector control design. The projected control method is implemented in MATLAB Power Systems and the outcome illustrate that the controller be capable of function under stable and changeable wind speed. Lastly a sensor less velocity estimator is in implementation which enables the wind turbine to drive without the perfunctory speed sensor. The simulation and investigational consequences for the sensor less speed estimator are obtainable*

**Keywords:** Synchronous Generator, IPM-Interior Permanent Magnet , Direct Control , Variable Speed Wind Turbine , Senseless Speed Estimator.

Copyright © 2017 International Journal for Modern Trends in Science and Technology  
All rights reserved.

## I. INTRODUCTION

Recent trend indicates that wind energy will play a major role to meet the future energy target worldwide to reduce reliance on fossil fuel and to minimize the adverse impact of climate change. Wind energy is the fastest growing generation technology among the renewable energy sources. Over the last decade, the global wind energy capacity has increased rapidly and wind is an important competitor to the traditional sources of energy. In 2013, more than 35 GW of wind power capacity was added to the global wind generation capacity which became 318 GW .Since 2008 annual growth rates of cumulative wind power

capacity have averaged 21.4%, and global capacity has increased eightfold over the past decade. Recently, capital costs of wind generation technologies have declined primarily due to the competition and advanced technology development including taller towers, longer blades, and smaller generators in low wind speed areas have increased capacity factors. The technological development contributed to reduce the costs of wind turbines and made it competitive relative to fossil fuel based generation. Onshore wind-generated power is now more cost competitive on a per kWh basis with new coal/gas fired power plants, in several markets (including Australia, Brazil, Chile, Mexico, New Zealand, South Africa, Turkey, much of the EU, and some locations in India and the United States).

As a result of this trend, high level of wind energy (>30%) will be integrated into the power grid and major challenges and issues will appear, which are needed to be addressed for efficient and reliable operation of the existing power system.

As the wind penetration increases, the structure and dynamics of the power system network will change significantly over the coming decades. Due to the intermittent nature of wind power, the replacement of traditional synchronous generators with power electronic converter-based synchronous generators will introduce special challenges in grid interconnections and bi-directional power control, tight voltage and frequency regulation, dynamic stability, low voltage fault ride through, satisfy grid code, system security, reliability, and protection. Therefore, a better understanding of the technology involved with the grid integration of the variable speed wind turbines and possible impacts of large scale wind integration to the power grid is mandatory to ensure reliable and secure operation of the power system.

Over the last two decades, wind power has become the most promising renewable energy technology due the development in wind turbine aerodynamics, structure, variable speed generator technologies, power electronics and DSP (digital signal processor) based control topologies. The wind turbine industries is continuously moving forward in order to increase efficiency and controllability of the variable speed wind turbines to enhance the large scale grid integration of wind energy conversion system. Recent trend indicates an increase in large scale wind farms, which will contribute to significant share of the energy. They will also introduce new challenges and issues in the power system operation and control. These challenges include integration to the weaker grid, voltage and frequency regulation, dynamic voltage stability under disturbances, power fluctuations and changing dynamics of the conventional power plants. The wind farms will have to fulfil the new grid code requirement for reliable and stable operation of the power system. Currently, the doubly fed induction generator (DFIG) based gear-driven variable speed wind turbine technology dominating the market. However, there is an increasing trend for permanent magnet synchronous generator (PMSG) based gearless direct drive variable speed wind turbine due to superior performance, efficiency, smaller size, less maintenance and enhanced fault ride through capability.

Currently, variable-speed wind turbine technologies are very popular because of their Advantages such as increased energy capture, maximum power extraction, higher efficiency and better power quality. The majority of the current installed turbines use doubly fed induction generator (DFIG) based changeable speed wind turbines with gearbox as exposed in Fig.1.3 (a). The benefit of this technology is to facilitate it requires power converter with abridged capacity (30% of full capacity) as the converter is linked to the rotor circuit as a substitute of stator circuit. In this configuration, the stator is directly connected to the grid and the rotor is connected to grid through a power converter to control the rotor frequency and the rotor speed. Depending on the size of the frequency converter (usually rated at approximately 30% of nominal generator power) this technology can operates in a wide speed range. Typically, the variable speed range is  $\pm 30\%$  around the synchronous speed, which makes this concept attractive and popular from economic point of view. When the generator runs at super-synchronous speed, the electrical power is injected to the grid through both the rotor and the stator. When the generator runs at sub-synchronous speed, the electrical power is delivered into the rotor from the grid. Fig.1.3 (b) and Fig.1.3(c) show self-excited induction generator and wound rotor synchronous generator based gear driven variable speed wind turbines, respectively.

On the other hand, the major drawback of this category of wind turbine is the requirement of a gearbox which requires standard safeguarding and suffers from faults and malfunction. Furthermore it increases the on the whole size of the wind turbine. Another disadvantage of DFIG topology is that it is very sensitive to grid disturbance, especially for the voltage dip, due to the fact that the stator is directly connected to the grid. The voltage dip could cause over voltage and over current in the rotor windings and consequently damaged the rotor side converter. To provide a DFIG with good fault ride through (FRT) the wind turbine and the power converter should have the ability to protect itself, without disconnecting during faults. In order to fulfill this requirement, a crowbar is needed to offer extra protection to bypass the converter by short-circuiting the rotor windings.

In this configuration, the generator rotor is directly connected to the turbine rotor without any gearbox

and the generator is interfaced with the grid/load using full scale AC-DC-AC power converters as shown in Fig.1.4. This configuration is most suited for full power control as it is connected to the grid through a power converter. The permanent magnet synchronous generators (PMSGs) used in this configuration are low speed generators with suitable number of poles and able to produce higher torque at low speed. The full-scale power converter knows how to perform smooth grid association over the complete speed range. The power electronic converters used in this configuration have two primary goals: to act as an energy buffer (DC-link) for the power fluctuations caused by the wind turbine and for the transients coming from the grid side and enables the system to control active and reactive power.

The most important features of PMSG based wind turbines are

- a) Gearless function and enhanced reliability
- b) Uncomplicated structure, smaller size and reduced cost
- c) Small mechanical and electrical losses
- d) Superior power factor and efficiency
- e) No requirement for reactive power holds up
- f) elevated cost and power losses in the converters.
- g) No need of external excitation.

This type of wind turbine has a better fault ride through capability compared with the DFIG system with better efficiency and lesser complexity. Therefore, direct drive variable speed wind turbine is becoming more attractive. However, the reactive power requirements can be fulfilled through the power converter control for both DFIG and direct drive wind turbine with full scale converter concepts.

## II. PROCEDURE FOR MODELING OF WIND TURBINE

### A. Modeling of Wind Turbine and Maximum power extraction

The power confine by the wind turbine is specified by

$$P_m = 0.5AC_p(\lambda_r, \beta) \times (v_w)^3 = 0.5\rho AC_p \times (\omega_m R/\lambda_r)^3 \quad (1)$$

$\rho$  = Density of air (kg/m<sup>3</sup>)  $v_w$  =Velocity of wind (m/s)  $A$  = Area enclosed by turbine blades (m<sup>2</sup>)  $C_p$  = Power coefficient  $\omega_m$  = Speed at which turbine rotates  $R$  = radius of wind turbine blades. The power coefficient is a function of tip speed ratio ( $\lambda_r$ ) and pitch angle ( $\beta$ )

The tip speed ratio is set by

$$TSR = \lambda_r = \frac{\text{rotor tip speed}}{\text{wind speed}} = \omega_m R/v_w \quad (2)$$

The wind turbine can take out maximum power from wind only when  $C_p$  is at maximum value ( $C_{p\_opt}$ ).  $C_p$  value totally depends on  $\beta$  and  $\lambda_r$ . As a result, it is required to make the  $TSR(\lambda_r)$  value forever stays at an optimum value ( $\lambda_{r\_opt}$ ). If wind speed is unreliable, the turbine speed must be in tune consequently so as to see  $\lambda_r$  is at  $\lambda_{r\_opt}$ . we be capable of observing that maximum value of  $C_p$  is possible only when  $\beta = 0$  and as pitch angle increase, the maximum possible value of  $C_p$  decrease. So it is advantageous that  $\beta = 0$  in order to get maximum power extraction from the wind with superior efficiency. The objective optimum power from a wind turbine is given as

$$P_{m\_opt} = 0.5\rho AC_{p\_opt} ((\omega_{m\_opt} R)/\lambda_{r\_opt})^3 = K_{opt} (\omega_{m\_opt})^3 \quad (3)$$

Where

$$K_{opt} = 0.5\rho AC_{p\_opt} (R/\lambda_{r\_opt})^3 \quad (4)$$

And

$$\omega_{m\_opt} = \omega_{g\_opt} = (\lambda_{r\_opt} / R)v_w = K_w v_w \quad (5)$$

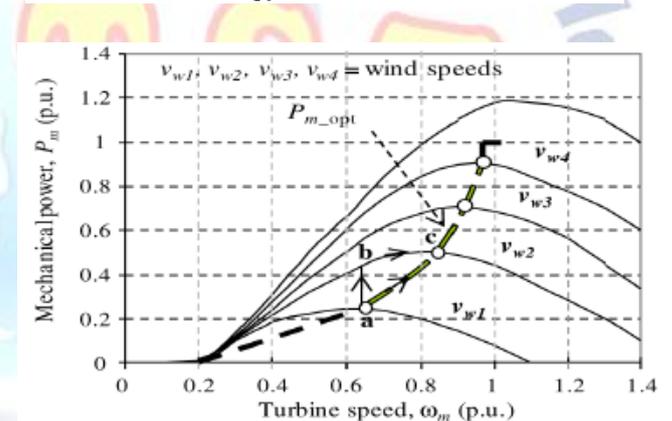


Fig:1 Mechanical power generated by the turbine as a function of the rotor speed for dissimilar wind speeds.

The optimum torque can be specified by

$$T_{m\_opt}(t) = K_{opt} [W_{m\_opt}(t)]^2 \quad (6)$$

Hence Optimum values are the values at which turbine can extract maximum energy from the unreliable wind speeds and thus create maximum power from the generator. The purpose of the controller is to keep the turbine operating on this curve, as the wind speed changes. There is always a matching rotor speed that produces optimum power for a particular wind speed. If the controller can properly follow the optimum curve, the wind turbine will make maximum power at any speed within the permissible range. The optimum torque can be designed from the optimum power given by (6).

### III. PROCEDURE FOR MODELING OF SYNCHRONOUS GENERATOR

The Permanent Magnet Synchronous Generator PMSG is on the whole principally wound rotor synchronous generator everywhere the rotor is replaced with permanent magnet. For the reason it is of permanent magnet, rotor does not necessitate any exciting current for maintaining air gap flux. Consequently the rotor excitation losses will not be present. So wind energy can be used proficiently for producing electric power. To examine IPM SG, the machine is modeled in d-q reference frame, which is synchronously rotates with the rotor; where d-axis is along the magnetic axis and q-axis is orthogonal to it is utilized. The d-axis and q-axis voltages of PMSG is specified by

$$v_d = -i_d R_s - \omega_r \lambda_q + p \lambda_d \quad (7)$$

$$v_q = -i_q R_s + \omega_r \lambda_d + p \lambda_q \quad (8)$$

The d- and q-axes flux linkages are given by

$$\lambda_d = -L_d i_d + \lambda_M \quad (9)$$

$$\lambda_q = -L_q i_q \quad (10)$$

The torque equation of the PMSG can be shown as

$$T_g = -\frac{3}{2}P(\lambda_d i_q - \lambda_q i_d) = -\frac{3}{2}P[\lambda_M i_q + (L_d - L_q)i_d i_q] \quad (11)$$

$R_s$  = Resistance of the stator.

$\omega_r$  = Speed at which generator rotates

$\lambda_M$  = Magnetic flux

$P$  = Pole pairs

$p$  =  $d/dt$  operator

In equation (7)–(11)  $v_d$ ,  $v_q$ ,  $i_d$ ,  $i_q$ ,  $L_d$  and  $L_q$  are the d- and q-axes stator voltages, currents, and inductances, correspondingly. The dq model of IPM synchronous generator is made known in Fig.2

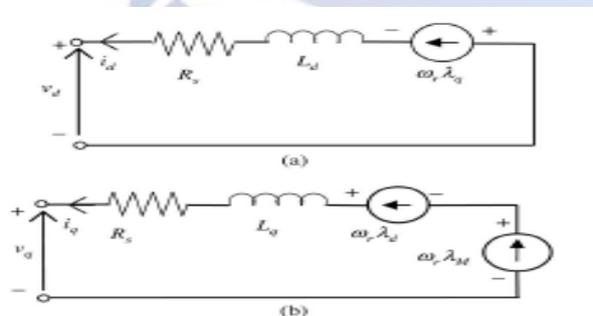


Fig.2. dq-model of IPM synchronous generator: (a) d-axis equivalent circuit and (b) q-axis equivalent circuit.

The initial term in the torque equation (11) is the excitation torque that is formed by the interaction

of permanent magnet flux  $i_q$  and is self-governing of  $i_d$ . The subsequent term is the reluctance torque that is relative to the product of  $i_d$  and  $i_q$  to the distinction between  $L_d$  and  $L_q$ . For the surface PMSG, the reluctance torque is zero since  $L_d=L_q$ , at the same time as for the IPM synchronous generator, superior torque can be induced for the same  $i_d$  and  $i_q$ , if  $(L_d-L_q)$  is better. This is one of the compensation of IPM synchronous generator over surface PMSG

The d- and q-axes current reference can be articulated as

$$i_q^* = \frac{2T_g^*}{3P[\lambda_M + (L_d - L_q)]i_d} \quad (12)$$

$$i_d^* = \frac{\lambda_M}{2(L_d - L_q)} - \sqrt{\frac{\lambda_M^2}{4(L_d - L_q)} + (i_q^*)^2} \quad (13)$$

A range of parameters of PMSG considered for simulation analysis is given in Table-1

TABLE-1

Rated power	4Kw
Rated torque	24Nm
Rated speed	1600 rpm
Rated voltage	415 V rms
Rated current	9.6 A rms
Magnetic flux linkage	0.525723Wb
d-axis inductance ( $L_d$ ) per phase	18.237mH
q-axis inductance ( $L_q$ ) per phase	0.0049 kg-m2
Stator resistance	1.56 ohms
No.of poles	6
Static friction	0.637 Nm
Viscous damping	0.237 Nm/krpm

### IV. PROJECTED AND PROPOSED DIRECT CONTROL SCHEME FOR INTERIOR PERMANENT MAGNET SYNCHROUS GENERATOR

In the projected and proposed direct control scheme, current controllers are not used. as an alternative, the torque and stator flux can be synchronized independently and directly by using two separate hysteresis controller bands for flux as well as torque. This control scheme for IPM synchronous generator is exposed in Fig. 3.

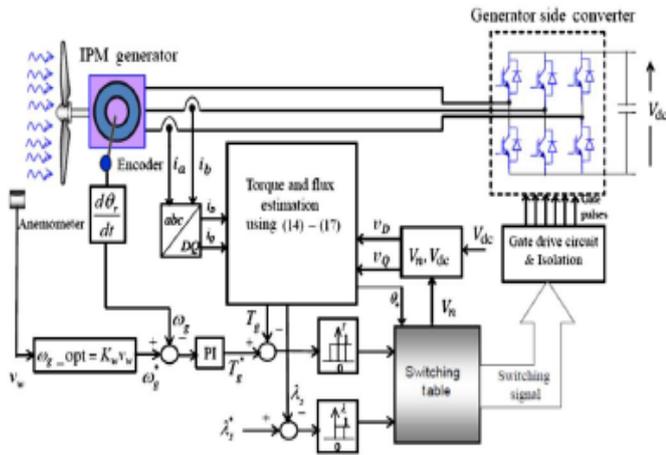


Fig: 3 Planned and Proposed direct control scheme

The assortment rule is made in such a way that errors there in torque and flux will be inside the hysteresis bands so as to acquire the required flux and torque response. The necessary voltage vectors for switching the converter are chosen according to the switching table as revealed in Table-2 the assortment of the voltage space vectors can be resolved by the position of the stator flux linkage vector and the outputs of the two hysteresis comparators. The hysteresis control blocks evaluate the torque and flux references with predictable torque and flux, correspondingly. When the estimated torque/flux drop at a level below its differential hysteresis limit, the torque/flux status output goes high elevated.

TABLE-2

$\theta$		$\theta_1$	$\theta_2$	$\theta_3$	$\theta_4$	$\theta_5$	$\theta_6$
$\lambda$	$\tau$						
	$\tau=1$	$V_2(110)$	$V_3(010)$	$V_4(011)$	$V_5(001)$	$V_6(101)$	$V_1(100)$
$\lambda=1$	$\tau=0$	$V_6(101)$	$V_1(100)$	$V_2(110)$	$V_3(010)$	$V_4(011)$	$V_5(001)$
	$\tau=1$	$V_3(010)$	$V_4(011)$	$V_5(001)$	$V_6(101)$	$V_1(100)$	$V_2(110)$
$\lambda=0$	$\tau=0$	$V_5(001)$	$V_6(101)$	$V_1(100)$	$V_2(110)$	$V_3(010)$	$V_4(011)$

After the estimated torque/ flux rise above differential hysteresis limit, the torque/flux output goes small. The differential limits, switching points for mutually torque and flux, are determined by the hysteresis band width. The suitable stator voltage vector can be preferred by using the switching logic to persuade both the torque and flux status outputs. At hand there are six voltage vectors and two zero voltage vectors that a voltage source converter can construct. The amalgamation of the hysteresis control block (torque and flux comparators) and the switching logic block

eliminate the need for a traditional PWM modulator. The most favorable switching logic is based on the mathematical spatial relationships of stator flux, rotor flux, stator current, and stator voltage. And the stator flux linkage is projected as.

$$\lambda_D = - \int (v_D - i_D R_s) dt \quad (14)$$

$$\lambda_Q = - \int (v_Q - i_Q R_s) dt \quad (15)$$

The stator flux linkage equation is agreed as

$$\lambda_s = \sqrt{\lambda_Q^2 + \lambda_D^2} \text{ and } \theta_s = \tan^{-1}(\lambda_Q / \lambda_D) \quad (16)$$

The electromagnetic torque can be designed by using

$$T_g = -\frac{3}{2} P (\lambda_D i_Q - \lambda_Q i_D) \quad (17)$$

The torque equation in terms of generator parameters is specified by

$$T_g = -\frac{3P\lambda_s}{4L_d L_q} (2\lambda_M L_q \sin \delta - \lambda_s (L_q - L_d) \sin 2\delta) \quad (18)$$

## V. SELECTION OF APPROPRIATE STATOR VOLTAGE VECTOR TO CONTROL STATOR FLUX LINKAGE

The stator voltages for a three phase machine in the outline of voltage vector is prearranged by

$$v_s = \frac{2}{3} (v_a + v_b e^{j2\pi/3} + v_c e^{j4\pi/3}) \quad (19)$$

According to the wind speed variations, it is desirable to control the switches of generator side converter. At this point, we are using the ideal bidirectional switches correspond to the power switches with their anti parallel diodes. The principal voltages are determined by the statuette of these three switches revealed in Fig.4

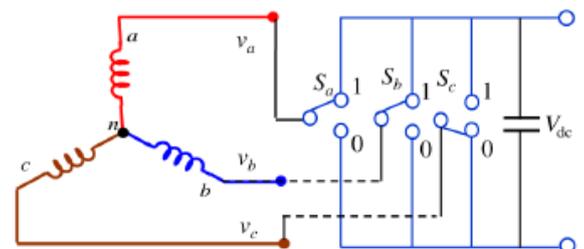


Fig. 4. Rectifier connected to IPM synchronous generator

Through making the use of a series of switches, from the 3 input legs, AC is transformed into a controlled DC. At this juncture total of eight

switching vectors are potential for the rectifier, in that 6 are active switching vectors and 2 are zero vectors depending on the point of these 3 switches (Sa, Sb, Sc), the principal voltage vectors va, vb, vc are definite. The 6 non-zero voltage vectors are to displace 60° from one another. These eight voltage vectors can be written in single equation at the same time as

$$v_s(S_a, S_b, S_c) = V_D(S_a + S_b e^{j2\pi/3} + S_c e^{j4\pi/3}) \quad (20)$$

Wherever  $V_D = 2/3V_{dc}$  and  $V_{dc} = \text{dc-link voltage}$

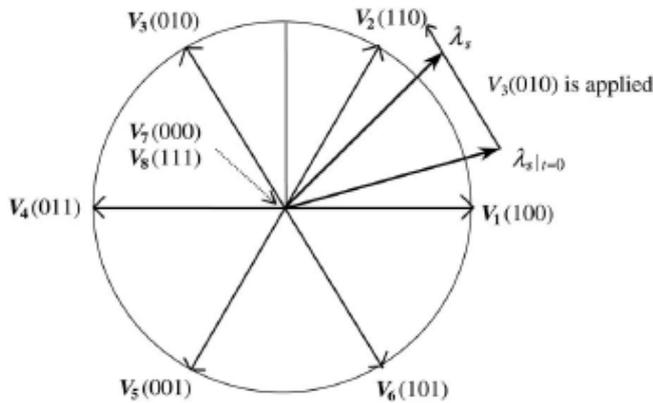


Fig. 5 Vectorial representations of the stator voltage vectors.

Within equation (20), by substituting values of switching states, we can discover the values of these 6 non-zero voltage vectors. These voltage vectors can be signify as in table -3

TABLE - 3

V1	V2	V3	V4	V5	V6
VD	VD	0.5VD	-0.5VD	-VD	0.5VD
VQ	0	0.866VD	0.886VD	0	-0.886VD

VOLTAGE VECTOR VALUES

#### A. Control of Amplitude of stator flux linkages

The stator flux linkage in the stationary orientation frame can be specified as

$$\lambda_s = \int (v_s - i_s R_s) dt. \quad (21)$$

Above equation can be made to rewrite as

$$\lambda_s = v_s t - R_s \int i_s dt. \quad (22)$$

The above equation is to make performance that the tip of the stator flux linkage vector  $\lambda_s$  will shift in the direction of the applied voltage vector. How remote the tip of the stator flux linkage will shift is resolute by the duration of time for which the stator vector is applied is given away in Fig. 6. The area to control magnitude and direction of the stator flux, the vector plane of the voltages is made to partition into six regions  $\theta_1$ – $\theta_6$  in order to choose the requisite voltage vectors of the converter to control the amplitude and direction of the stator flux. In each area, two neighboring voltage vectors have to be selected depending on hysteresis commands. While  $\lambda_s$  is in region  $\theta_1$ , V2 is selected to reduce the amplitude of  $\lambda_s$  and V3 is selected to augment the amplitude of  $\lambda_s$ . That way amplitude of  $\lambda_s$  is controlled by making error value to stay within hysteresis band limits. Here these ways, the controller mechanism by choose the switching vectors properly for the converter.

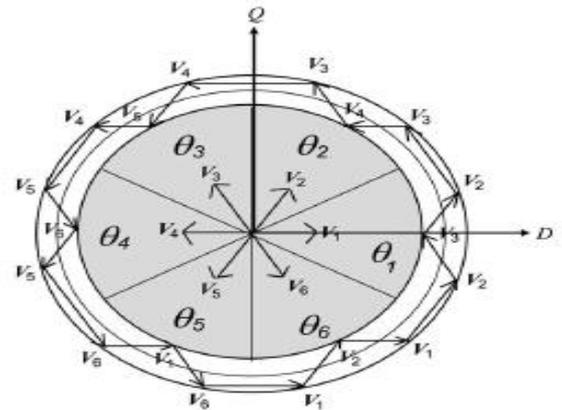


Fig. 6. Control of the magnitude and the direction of the stator flux

#### B. Control Rotation of Stator Flux linkage ( $\lambda_s$ )

By means of controlling the direction of rotation of  $\lambda_s$ , the electromagnetic torque is capable of controlled; this is with high opinion to the equation (18). In anti-clockwise functioning, if the torque error is positive that means real is less than reference, the suitable switching vectors are selected for that reason to build  $\lambda_s$  rotate in the same direction. This makes  $\theta$  to reduce and so actual torque to boost.  $\lambda_s$  rotates in the similar direction till the real torque become more than the orientation torque. As soon as actual torque is more than the reference, error becomes negative and voltage vectors of opposite axes are preferred to keep  $\lambda_s$  rotating in the reverse direction. This makes  $\theta$  to reduce and so real torque to diminish. By pick the switching vectors in this pattern,  $\lambda_s$  is rotated in all directions and the rotation of  $\lambda_s$  is

controlled by the commands specified by the torque hysteresis controller.

The consequence of two nonzero voltage vectors V7 and V8 is more complex. It is seen from (22) that  $\lambda_s$  will settle at its original position when zero voltage vectors are functional. This is accurate for induction machine given that the stator flux linkage is exceptionally determined by the stator voltage, wherever the rotor voltages are always zero. In the case of an IPM synchronous generator,  $\lambda_s$  will alter even when the zero voltage vectors are practical, because magnet flux  $\lambda_s$  continues to be supplied by the rotor and it will rotate with the rotor. In supplementary words,  $\lambda_s$  should for all time be in motion with respect to the rotor flux linkage. The voltage vector switching table to control the amplitude as well as direction of  $s$  is known in Table -3  $\lambda$  and  $\tau$  denotes the hysteresis controller outputs of stator flux and torque, correspondingly.

### VI. A NOVEL DIRECT CONTROL PROCEDURE FOR INTERIOR PERMANENT MAGNET SYNCHRONOUS GENERATOR BASED WIND TURBINE

The direct control procedure for IPM synchronous generator is made known in Fig. 3, where the switching method used is exposed in Table -3. The three-phase variables are changed into stationary DQ-axes variables. As exposed in Table-2, torque error and flux error are the inputs to the flux hysteresis comparator and torque hysteresis comparator, in that order. The outputs of the hysteresis comparators ( $T$ ,  $\lambda$ ) are the inputs to the voltage-switching assortment research table. As shown in Fig. 3, this proposal is not dependent on generator parameters apart from the stator resistance. Furthermore, all calculations are in the stator DQ orientation frame and without any co-ordinate alteration. The DQ-axes flux linkage components  $\lambda_Q(k)$  and  $\lambda_D(k)$  at the  $k$  th sampling immediate is specified by

$$\lambda_{Q(k)} = T_s [-v_{Q(k-1)} + R_s i_{Q(k)}] + \lambda_{Q(k-1)} \quad (23)$$

$$\lambda_{D(k)} = T_s [-v_{D(k-1)} + R_s i_{D(k)}] + \lambda_{D(k-1)} \quad (24)$$

Wherever  $T_s$  is the sampling time, the variables with subscript  $K$  are their values at the  $K$  the sampling instantaneous, and the variables with  $K-1$  are the preceding sample. The DQ -axes currents can be made obtain from the measured three-phase currents and the DQ-axes voltages are designed from the measured dc-link voltages. Table -2 shows  $V_d$  and  $V_q$  axes voltages for the applied voltage vectors. The magnitude of the stator flux linkage is planned by

$$\lambda_s(k) = \sqrt{\lambda_{D(k)}^2 + \lambda_{Q(k)}^2} \text{ and } \theta_s = \tan^{-1}(\lambda_{Q(k)}/\lambda_{D(k)}) \quad (25)$$

The torque developed is known by

$$T_g(k) = -\frac{3}{2} P (\lambda_{D(k)} i_{Q(k)} - \lambda_{Q(k)} i_{D(k)}) \quad (26)$$

The generator developed torque, in terms of stator and rotor flux linkage amplitudes, is also prearranged by

$$T_g(k) = -\frac{3P\lambda_s(k)}{4L_d L_q} \times [2\lambda_M L_q \sin\{\delta(k)\} - \lambda_s(k)(L_q - L_d) \sin 2(\delta(k))]$$

### VII. IPM DIRECT CONTROL SIMULATION MODEL

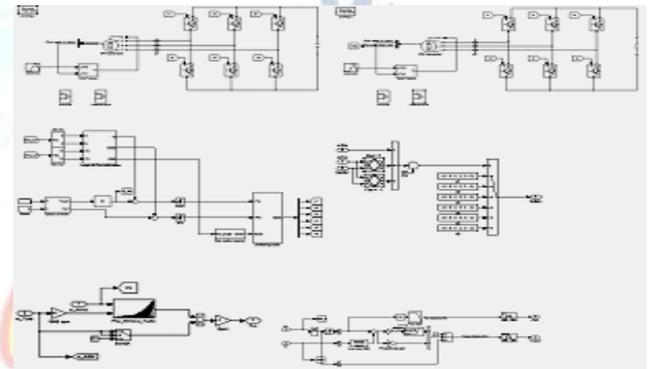


Fig. 7. Matlab/ Simulink model for IPM direct control proposal

### VIII. SIMULATION RESULTS

With changeable wind speed routine of this direct control technique is experimental. It has been observed that for varying wind speeds, torque, flux, turbine speed are subsequent to the references revealed in fig. 7 is to implement in MATLAB Power systems dynamic system simulation software. For comparison, the traditional vector-controlled scheme revealed in Fig.8 has also been put to implement in MATLAB/Simulink Power Systems using the identical IPM synchronous generator. MATLAB/Simulink Power Systems wind turbine model is used in this job. The contribution input to the wind turbine model is wind speed and the productivity output is torque

#### A. Performance of indirect vector Control scheme

The near perfection performance by the indirect vector control of IPM synchronous generator based variable speed wind turbine. The d-axes and q-axes currents and their references are shown in Fig 8(b) and (c) in that order and the wind speed in Fig 8(a). It is being seen that d-axes and q-axes currents go behind their references quite well and regulate the generator current under diverse wind speeds. As given away in Fig 8(d) the speed controller is proficient to regulate the speed for unreliable wind speeds

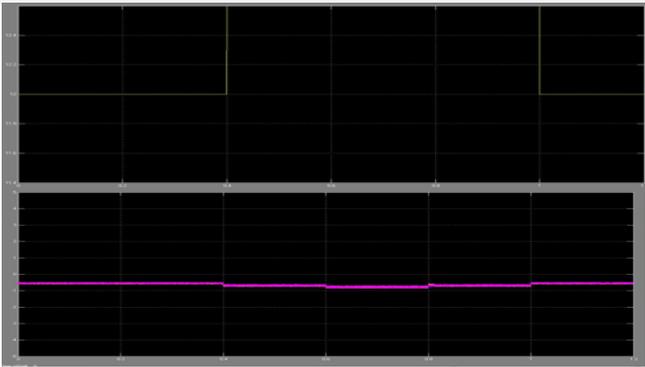


Fig: 8 Performance of the traditional indirect vector control scheme: (a) wind speed, (b) d-axis current and its position

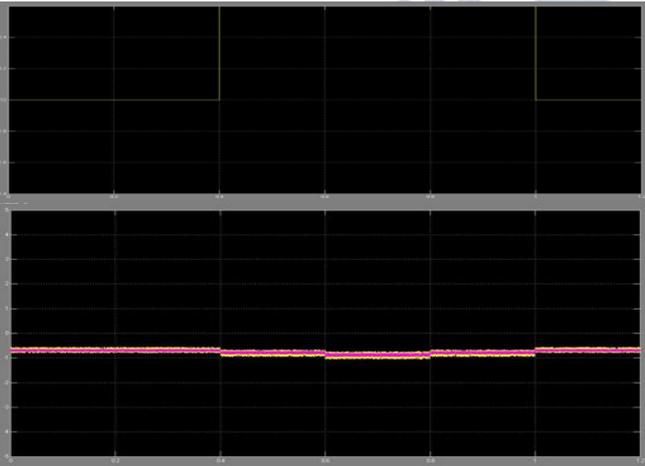


Fig: 8 Performance of the traditional indirect vector control scheme: q-axis current and its reference, and (d) speed orientation and deliberate speed.

### B. Performance of Direct Torque and Flux Control Scheme

The near accurate performance of direct control scheme for IPM synchronous generator based variable speed wind turbine. Fig. 9(a)–(d) shows the wind speed, torque reaction, flux linkage response, and speed response, correspondingly. As revealed in Fig. 9(b) and (c), the torque and flux linkages are subsequent these reference quite well and regulate the torque and flux of the generator at different wind speeds. Fig. 9(d) shows the speed response, where the considered speed follows the reference speed well and the speed controllers regulate the generator speed under unreliable wind circumstances.

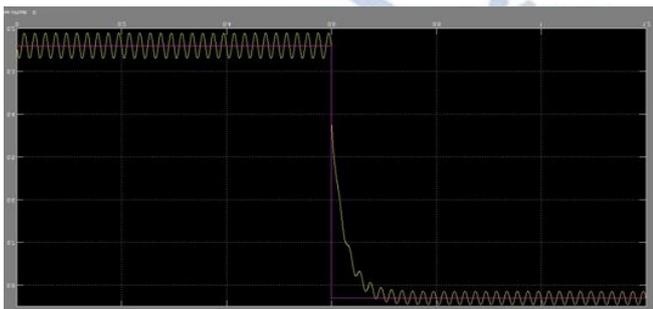


Fig: 9 Performance of the direct control scheme: (a) Wind speed, (b) torque and its reference

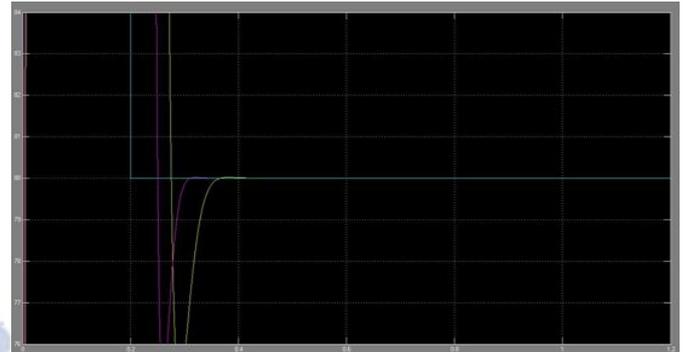


Fig: 9 Performance of the direct control scheme: (c) Flux linkage and its reference, and (d) speed reference and measured

## IX. CONCLUSION

Here this paper projected a sensor less novel direct control policy for an IPM synchronous generator-based variable speed wind turbine. During this control method, no rotor situation is required as all the calculations are done in stator orientation frame. The planned direct control system possesses quite a few advantages compared among indirect vector control method a) the smaller parameter reliance b) the torque and flux control devoid of rotor position and PI controller which decrease the linked delay in the controllers and c) sensor less action lacking mechanical sensor. The consequences illustrate that the direct controller can function beneath unreliable wind speeds. On the other hand direct control method has the difficulty of superior torque ripple that be able to bring in speed ripples and lively shaking in the power train. The technique to diminish the torque/ speed ripples wants to be address. The replication and investigational consequences for the sensor less speed estimator are accessible, and the outcome explains that the estimator can approximate the generator speed moderately well with an extremely minute fault.

## REFERENCES

- [1] S. Müller M. Deicke and R. W. D. De Doncker Doubly fed induction generator system for wind turbines IEEE Ind. Appl. Mag., vol. 8, no. 3, pp. 26–33, May 2002.
- [2] J. Hu, H. Nian, H. Xu, and Y. He, Dynamic modeling and improved control of DFIG under distorted grid voltage conditions IEEE Trans. Energy Convers., vol. 26, no. 1, pp. 163–175, Mar. 2011.
- [3] M. Mohseni, M. S. M. Islam, and M. A. Masoum, Enhanced hysteresisbased current regulators in vector control of DFIG wind turbine IEEE Trans. Power Electron., vol. 26, no. 1, pp. 223–234, Jan. 2011.

- [4] H. Polinder, F. F. A. Van der Pijl, G. J. de Vilder, and P. J. Tavner, Comparison of direct-drive and geared generator concepts for wind IEEE Trans. Energy Convers., vol. 3, no. 21, pp. 725–733, Sep. 2006.
- [5] T. F. Chan and L. L. Lai Permanent-magnet machines for distributed generation: A review IEEE Power Engg. Annual Meeting, Tampa, FL, USA, Jun. 24–28, 2007, pp. 1–6.
- [6] M. E. Haque, M. Negnevitsky, and K. M. Muttaqi, “A novel control strategy for a variable-speed wind turbine with a permanent-magnet synchronous generator,” IEEE Trans. Ind. Appl., vol. 46, no. 1, pp. 331–339, Jan./Feb. 2010.
- [7] R. Esmali and L. Xu, Sensorless control of permanent magnet generator in wind turbine application IEEE Industry Applications Society Annual Meeting, Tampa, FL, USA, Oct. 8–12, 2006, pp. 2070–2075.
- [8] M. Chinchilla, S. Arnaltes, and J. C. Burgos, Control of permanent-magnet generators applied to variable-speed wind-energy systems connected to the grid,” IEEE Trans. Energy Convers vol. 21, no. 1, pp. 130–135, Mar. 2006.
- [9] S. M. Deghan, M. Mohamadian, and A. Y. Varjani, A new variable-speed wind energy conversion system using permanent-magnet synchronous generator and Z-source inverter IEEE Trans. Energy Convers, vol. 24, no. 3, pp. 714–724, Sep. 2009.
- [10] S. Morimoto, H. Nakayama, M. Sanada, and Y. Takeda Sensorless output maximization control for variable-speed wind generation system using IPMSG IEEE Trans. Ind. Appl., vol. 41, no. 1, pp. 60–67, Jan./Feb. 2005.
- [11] W. Qiao, L. Qu, and R. G. Harley Control of IPM synchronous generator for maximum wind power generation considering magnetic saturation IEEE Trans. Ind. Appl., vol. 45, no. 3, pp. 1095–1105, May/Jun. 2009.
- [12] C. N. Bhende, S. Mishra, and S. G. Malla Permanent magnet synchronous generator based standalone wind energy supply system IEEE Trans. Sustain. Energy, vol. 2, no. 4, pp. 361–373, Oct. 2011.
- [13] S. Zhang, K. J. Tseng, D. M. Vilathgamuwa, T.D. Nguyen, and X. Y. Wang Design of a robust grid interface system for PMSG-based wind turbine generators IEEE Trans. Ind. Electron., vol. 58, no. 1, pp. 316–328, Jan. 2011.
- [14] A. Uehara, A. Pratap, T. Goya, T. Senjyu, A. Yona, N. Urasaki, and T. Funabashi A coordinated control method to smooth wind power fluctuation of a PMSG-based WECS IEEE Trans. Energy Convers., vol. 26, no. 2, pp. 550–558, Jun. 2011